Surface Molecular Motion of the Monodisperse Polystyrene Films

Tisato Kajiyama,*,† Keiji Tanaka, and Atsushi Takahara

Department of Chemical Science & Technology, Faculty of Engineering, Kyushu University, 6-10-1 Hakozaki, Higashi-ku, Fukuoka 812-81, Japan

Received April 18, 1996; Revised Manuscript Received August 9, 1996[⊗]

ABSTRACT: Forced modulation scanning force microscopic (SFM) and lateral force microscopic (LFM) measurements of the monodisperse polystyrene (PS) films were carried out at 293 K in order to reveal surface molecular motion. Surface dynamic storage modulus, E', and surface loss tangent, tan δ, of the monodisperse PS films were evaluated on the basis of forced modulation SFM measurement. It was revealed that the magnitudes of surface E' and surface tan δ were lower and higher than those for its bulk state, respectively, in the case of the number-average molecular weight (M_n) lower than 26.6k. Based on forced modulation SFM measurements, the surface of the PS film with M_n lower than 26.6k was in a glass−rubber transition state even at 293 K, in spite of that the bulk T_g was far above 293 K. LFM measurements for the PS films revealed that the magnitude of lateral force was dependent on the scanning rate of the cantilever tip in the case of M_n lower than 40.4k. The scanning rate dependence of lateral force appeared in the case that the surface of the PS film was in a glass−rubber transition state. LFM results agreed well with forced modulation SFM ones if the scanning rate of the cantilever tip for LFM measurement was converted to the measuring frequency for forced modulation SFM measurement. The active thermal molecular motion on the polymeric surface was explained by the excess free volume induced due to the surface localization of chain end groups. The surface enrichment of chain end groups was confirmed by dynamic secondary ion mass spectroscopic measurement.

Introduction

For the past a few years, the investigation of surface molecular motion for the polymeric materials has been paid great attention as well as the study of surface structure, due to its importance in various practical applications such as permselective membranes, biomaterials, adhesives, lubricants, and so on.[1−9] The authors investigated the depth dependence of the surface glass transition temperature, T_g for the poly(styrene-*block*-methyl methacrylate) diblock copolymer (P(St-*b*-MMA)) films on the basis of temperature and angular dependent X-ray photoelectron spectroscopic (XPS) measurements.[8,9] It was revealed that the surface T_g was much lower than that for its bulk sample and, also, the surface T_g gradually increased to the bulk T_g with an increase in the depth from the air−polymer interface. In the depth range from the top surface to 2.7 nm, the molecular weight dependence of the surface T_g for the P(St-*b*-MMA) film was more pronounced than that for its bulk sample and was expressed as $T_g = T_{g,\infty} - CM_n^{-(0.45\pm0.02)}$, where $T_{g,\infty}$ and M_n were T_g at infinite molecular weight and number-average molecular weight, respectively, whereas, on the basis of the scaling analysis on the assumption that the chain end groups are preferentially localized at the air−polymer interface, the molecular weight dependence of the surface T_g can be expressed as $T_g = T_{g,\infty} - CM_n^{-0.5}$.[6] Therefore, it seems reasonable to conclude from the magnitudes of the exponents mentioned above that the depression of T_g at the film surface is attributed to an increase in the free volume fraction which was induced mainly from the surface localization of chain end groups. Also, a little discrepancy of the molecular weight dependence of T_g between the experimental result and theoretical expectation might be interpreted by the additional activation of thermal molecular motion for polymeric chains due to its geometrically unsymmetrical environment at the air−polymer interface.[9] In our paper, "surface" is roughly defined as the region from the air−polymer interface to the depth of twice the radius of gyration of an unperturbed chain, $2R_g$.[8,9]

Scanning force microscopy (SFM) is one of the new scanning probe microscopy techniques and is important for investigating the surface morphology of materials with high resolution.[10−12] The SFM image was created on the basis of the various forces acting between the cantilever tip and sample surface such as van der Waals, electrostatic, frictional, magnetic, and so on. When the SFM observation is carried out in a repulsive force region of the force curve, the sample surface might be deformed by the indentation of a tip. The modulation of the indentation leads to the modulation of the force acting between the sample surface and cantilever tip. If the modulation of the tip indentation is applied sinusoidally to the sample surface, the dynamic viscoelastic properties at the sample surface can be evaluated by measuring the amplitude of the modulated deformation for the sample (response stress) and the phase lag between the modulation signal (stimulation strain) and modulated deformation signal (response stress).[13−16] The forced modulation SFM was designed by remodeling a commercially available SFM.[7] Although the two-dimensional mapping of dynamic mechanical properties for the phase-separated surface was performed by utilizing forced modulation SFM, the quantitative evaluation of the surface dynamic viscoelastic properties has not been done yet.[17−19]

The lateral force microscope (LFM) is also a useful tool for the two-dimensional mapping and/or the measurement of lateral force, which is evaluated by detecting the torsion of the sliding cantilever.[15,20] Lateral force measured by this technique is the sum of frictional and adhesion forces acting between the sample surface and cantilever tip.[21] Since frictional force greatly depends on the relaxation behavior of polymeric materi-

† Tel: +81-92-642-3558. Fax: +81-92-651-5606. E-mail: tkajitcf@mbox.nc.kyushu-u.ac.jp.

⊗ Abstract published in *Advance ACS Abstracts,* December 15, 1996.

S0024-9297(96)00582-7 CCC: $14.00

Table 1. Characterizations of PS Used in This Study

M_n	M_w/M_n	M_n	M_w/M_n
1.7k	1.09	26.6k	1.09
2.7k	1.10	40.4k	1.08
4.9k	1.08	47.5k	1.05
7.5k	1.09	140.0k	1.06
9.0k	1.09	218.6k	1.04
19.7k	1.07	1800k[a]	<1.30

[a] Purchased from Pressure Chemical Co., Ltd.

als,[22,23] it becomes possible to investigate the surface molecular motion on the basis of the scanning rate dependence of lateral force.[24] The purpose of this study is to investigate the surface molecular motion for the monodisperse PS films on the basis of forced modulation SFM and LFM measurements.

Experimental Section

Materials and Film Preparation. Monodisperse PSs were prepared by a living anionic polymerization at 293 K using *sec*-butyllithium as an initiator. Table 1 shows the number-average molecular weight, M_n, and the molecular weight dispersity, M_w/M_n, where M_w is the weight-average molecular weight. M_n and M_w/M_n were determined via gel permeation chromatography (GPC) with polystyrene standards. Bulk T_g was evaluated on the basis of differential scanning calorimetric (DSC) measurement at a heating rate of 10 K·min^{-1} under a dry nitrogen purge. The PS film of ca. 200 nm thick was coated from a toluene solution onto a cleaned silicon wafer by a spin-coating method at 2 krpm.

Setup of Forced Modulation SFM. Figure 1 shows the block diagram of the forced modulation SFM apparatus. The SFM equipment used in this study is an SPA 300 (Seiko Instruments Industry Co., Ltd.) with an SPI 3700 controller. The specimen is mounted on an *XYZ* piezoelectric scanner with a 20 μm scan range which has a resonance frequency of 15 kHz. The *Z*-sensitivity of the piezoelectric scanner is 4.46 nm·V^{-1}. The cantilever tip is mounted on the piezoelectric bimorph actuator which has a resonance frequency of 1−10 kHz depending on the applied electric field. The bimorph consists of alternating layers of metal electrodes, dielectric films, and piezoelectric zinc oxide films and can be bent vertically by applying the opposite electric field in the upper and lower piezoelectric sections.[25] The cantilever position in the *Z*-direction is modulated sinusoidally by applying an ac electric field, which is generated by the frequency generator (OSC), to the piezoelectric bimorph actuator. The deflection of the cantilever is measured by a position-sensitive four-segment photodiode (PSD) and feeds into the feedback loop that controls the height of the specimen. The modulated force is detected by the deflection of the cantilever. The deflection signal obtained with the PSD is filtered by a band-pass filter (BPF) in order to reduce the high- and low-frequency noises and feeds into a two-phase lock-in amplifier. The reference signal used is the sinusoidal signal from OSC which corresponds to the dynamic strain signal.

Evaluation of Surface Dynamic Viscoelastic Properties. The surface dynamic viscoelastic functions of the monodisperse PS film were evaluated on the basis of forced modulation SFM measurement. The distance between the tip and the sample surface was greatly influenced by the thermal drift of the piezoelectric scanner. Thus, the force and sample position cannot be evaluated precisely. Also, in our forced modulation SFM measurement, the bimorph at the other end of cantilever tip is modulated sinusoidally as shown in Figure 1. Thus, although the modulation amplitude of the bimorph can be evaluated accurately, the modulation amplitude of the cantilever tip cannot be determined precisely. However, in order to simplify the analysis, it was assumed that the magnitude of the modulation amplitude for the tip was same as that for the bimorph actuator.

The forced modulation SFM measurement was performed at 293 K in air under a repulsive force of ca. 25 nN. The modulation frequency and the modulation amplitude were 4 kHz and 1.0 nm, respectively. A commercially available silicon nitride (Si_3N_4) cantilever with integrated tips (Olympus Co., Ltd.) was used. The spring constant of the cantilever was 0.09 N·m^{-1}.

Lateral Force Measurement. In order to investigate the relaxation behavior of the PS film surface, LFM measurement was carried out at 293 K in air under a repulsive force of ca. 25 nN. LFM equipment used in this study was SPA 300 (Seiko Instruments Industry Co., Ltd.) with an SPI 3700 controller. The cantilever used in the LFM measurement was the same as that in the forced modulation SFM measurement. The magnitude of lateral force was evaluated by the line scan mode. Table 2 shows the scanning rate and the scanning distance measured in this study.

Investigation of Surface Localization of Chain End Groups. Depth profiling of the deuterated polystyrene (dPS) film of which chain end groups were labeled by protonated groups was carried out with dynamic secondary ion mass spectroscopic (DSIMS) measurement. Figure 2 shows the chemical structure of end-labeled dPS used in this study. End-labeled dPS was prepared by a living anionic polymerization. Only each end portion was labeled with proton. DSIMS analysis was performed using SIMS 4000 (Seiko Instruments Inc.-Atomika Analysetechnik GmbH). The incident beam of

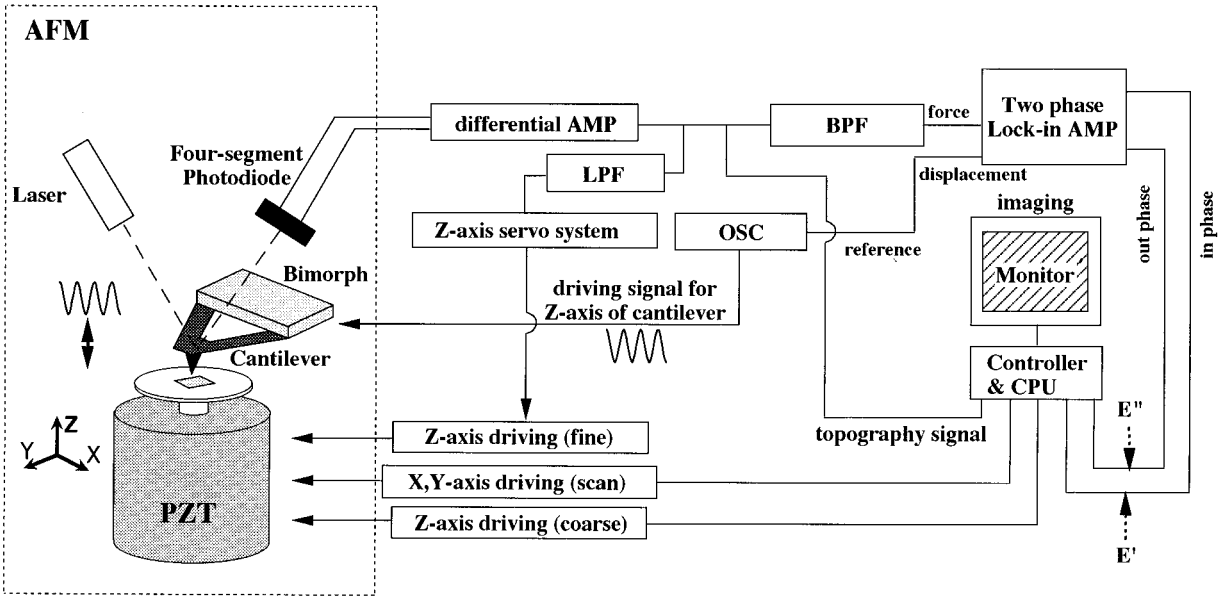

Figure 1. Block diagram of the forced modulation SFM equipment.

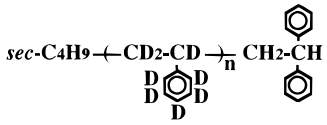

Figure 2. Chemical structure of end-labeled dPS.

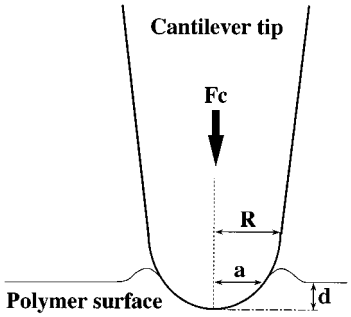

Figure 3. Model describing the surface deformation by the indentation of the tip.

Table 2. Condition for LFM Measurement Used in This Study

scanning rate/nm·s^{-1}	scanning distance/nm
1.0×10^2	3.91×10^2
2.5×10^2	9.84×10^2
6.0×10^2	1.18×10^3
1.0×10^3	9.83×10^2
2.5×10^3	1.23×10^3
6.0×10^3	2.95×10^3
1.0×10^4	2.46×10^3
3.5×10^4	6.14×10^3
6.0×10^4	7.37×10^3
1.0×10^5	1.23×10^4

oxgen ions with 3.0 keV and 6−7 nA was focused onto a 100 μm × 100 μm area of the specimen surface. A platinum layer of 10 nm thick was sputter-coated on the surface of the end-labeled dPS film in order to avoid a charging up of the specimen during the DSIMS measurement.

Results and Discussion

Molecular Weight Dependence of Surface Dynamic Viscoelasticity for the Monodisperse PS Film. When the modulated deformation with the amplitude up to ca. 5 nm was applied to the monodisperse PS film, the linear relationship between the amplitude of modulated deformation and the output voltage as a stress signal was observed.[26] Since our forced modulation SFM measurement was carried out under the condition with static deformation of 1.1 nm and dynamic deformation of 1.0 nm, the linear surface dynamic viscoelastic characteristics were investigated for the monodisperse PS film. Static deformation, that is, the indentation depth of the tip, was evaluated on the basis of Hertz' elastic theory.[27] Figure 3 shows the schematic representation of the surface deformation by the indentation of the tip. The indentation depth, d, of the tip was expressed as follows

$$d = \left[\frac{9}{16}\left(\frac{1-\mu_{\text{tip}}{}^2}{E_{\text{tip}}} + \frac{1-\mu_{\text{polymer}}{}^2}{E_{\text{polymer}}}\right)^2 F_c{}^2 R\right]^{1/3} \qquad (1)$$

where μ, E, R, and F_c are the Poisson ratio, modulus, the radius of curvature of the tip, and contact force, respectively. Since the tip is much harder than the sample, it is possible to neglect the first term in comparison with the second term in eq 1. The typical magnitudes of E and μ for the glassy PS are 4.5 GPa and 0.33, respectively. Also, R of 10 nm and F_c of 25 nN were used for the evaluation of d.

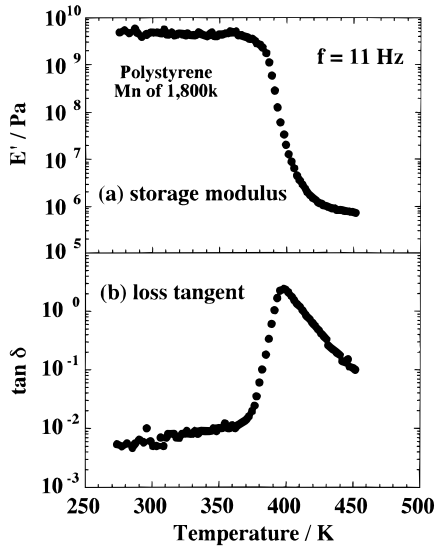

Figure 4. Temperature dependence of (a) bulk dynamic storage modulus, E', and (b) bulk loss tangent, tan δ, for the PS film with an M_n of 1800k as a standard. The measurement was performed at a frequency of 11 Hz by using Rheovibron.

Gaub et al. derived the surface dynamic storage modulus, E', and the surface loss modulus, E'', of the organic thin film in the case of forced oscillation SFM measurement with sample stage modulation.[14] Similarly, in the case of forced modulation SFM measurement with cantilever modulation, surface E' and surface E'' of the polymeric film can be expressed as follows

$$E' = (k_c H/\gamma)\langle(\cos\phi) - \gamma\rangle \qquad (2)$$

$$E'' = (k_c H/\gamma)\sin\phi \qquad (3)$$

where k_c, ϕ, and γ are a spring constant of the cantilever along the bent direction, an apparent phase lag between the force and the sample deformation, and a modulation ratio, respectively. Also, H is a parameter related to the contact area between the sample surface and probe tip and is called a shape factor. From eqs 2 and 3, surface loss tangent, tan δ, can be obtained by eq 4.

$$\tan\delta = E''/E' = \sin\phi/\langle(\cos\phi) - \gamma\rangle \qquad (4)$$

Since the magnitude of k_c is known and, also, the magnitudes of ϕ and γ are obtained experimentally, the magnitudes of E' and E'' can be determined after the magnitude of H is evaluated. The electrical and mechanical phase lags of the instruments were calibrated by using a silicon wafer as a standard with phase lag of zero.

The bulk dynamic viscoelastic properties for the PS film with a M_n of 1800k were measured with a Rheovibron (DDV01-FP, Orientec Co., Ltd.). Figure 4 shows the temperature dependence of bulk E' and bulk tan δ of the PS film with a M_n of 1800k. The α_a-dispersion behavior and the α_a-absorption peak corresponding to the micro-Brownian motion of a main chain was observed at ca. 390 K. The magnitudes of bulk E' and bulk tan δ for the glassy PS film at 293 K were evaluated to be 4.5 GPa and 0.005, respectively.

Parts a and b of Figure 5 show the molecular weight dependence of surface E' and surface tan δ of the

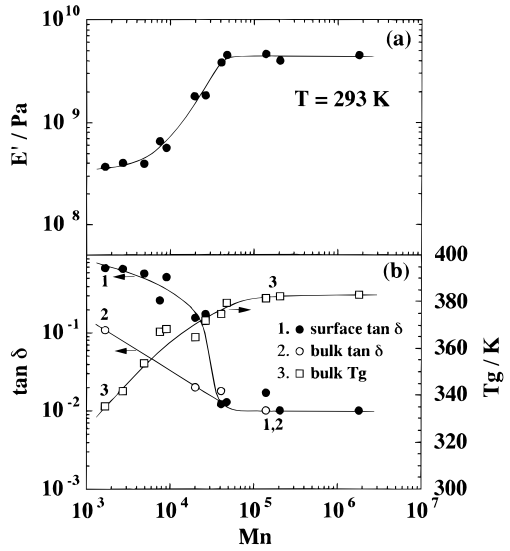

Figure 5. Molecular weight dependence of (a) surface dynamic storage modulus, E', and (b) surface loss tangent, tan δ, for the monodisperse PS film. The open circles and squares in (b) show bulk tan δ and bulk T_g, respectively.

monodisperse PS films as well as the bulk tan δ and bulk T_g values evaluated by DSC. Since the forced modulation SFM image of the monodisperse PS film was homogeneous, the image was not presented. Before the magnitude of H was determined, the M_n dependence of the output voltage as a stress signal was obtained. Since, in a higher M_n range from 40.4k to 1800k, the output voltage was almost constant, it can be considered that there is no M_n dependence on the magnitude of E', that is, the surface localization of chain ends is negligible. Especially, in the case of the PS film with a M_n of 1800k, since the concentration of the chain end group is extremely low, it seems reasonable to assume that thermal molecular motion at the film surface is comparable to that for the bulk sample even if chain end groups are preferentially segregated at the film surface. Then, on the assumption that the surface E' is the same as the bulk E' at 293 K, the magnitude of H can be decided. Since the magnitudes of the apparent phase lag between force and the sample deformation, ϕ, and the ratio of modulation amplitude, γ, were experimentally measured, the magnitudes of surface E' and surface tan δ for the PS film with each M_n were evaluated by using eqs 2 and 4. In a M_n range larger than 40.4k, the magnitudes of surface E' and surface tan δ were constant and their magnitudes were ca. 4.5 GPa and 0.01, respectively. Then, it seems reasonable to conclude from the magnitudes of surface E' and surface tan δ that the surface is in a glassy state at 293 K for the PS film with a M_n larger than 40.4k. Also, in the case of M_n smaller than 26.6k, as shown in Figure 5, the magnitudes of surface E' and surface tan δ decreased and increased with a decrease in M_n, respectively. The magnitudes of surface E' and surface tan δ indicate that the surface of the PS film with a M_n smaller than 26.6k is in a glass−rubber transition state even at 293 K. Dynamic viscoelastic properties of the monodisperse bulk PS sample were measured in order to compare the bulk E' with the surface E'. Since, in the case of M_n smaller than 40.4k, the film was very fragile, the dynamic spring analysis technique was applied to evaluate bulk tan δ.[28] In the case of M_n smaller than 26.6k, the magnitude of the surface tan δ was much higher than that of bulk tan δ, as shown in Figure 5b. This clearly indicates that the surface T_g of the PS film is more strongly dependent on M_n than the bulk T_g, because the M_n dependence of the surface tan δ is more apparent than that of bulk T_g. Thus, it seems reasonable to conclude that the thermal molecular motion at the film surface is more active in comparison with that for the bulk sample, especially in the case of M_n smaller than 26.6k.

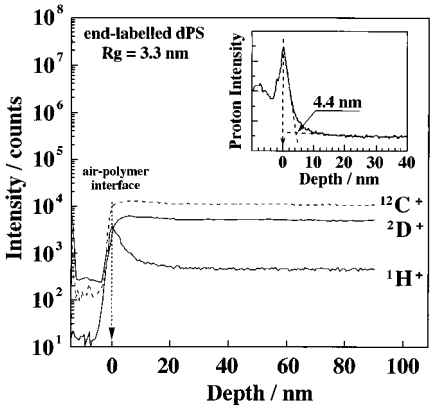

Figure 6. SIMS depth profile of proton, deuterium, and carbon ions for the end-labeled deuterated PS film. The inset enlarges the proton intensity profile in linear scale at the vicinity of the air−polymer interface. The depth before the attainment of the dashed vertical line corresponds to sputtering the etching of a platinum layer of 10 nm thick to avoid a charging of the specimen during SIMS measurement.

Surface Localization of Chain End Groups. A depression in T_g at the film surface compared with that for the bulk sample has been explained by the surface localization of chain end groups.[6,9] However, the relationship between the surface localization of chain end groups and the surface molecular motion has not been experimentally confirmed. Deuterated polystyrene (dPS) of which chain end groups were labeled by protonated groups was prepared and SIMS depth profiling was performed in order to confirm the surface localization of chain end groups.

Figure 6 shows the typical SIMS depth profile of the end-labeled dPS film. The dashed vertical line corresponds to the air−polymer interface. The intensity of the carbon ion, C^+, was almost constant at any depth position from the polymer film surface and the steady-state etching proceeded during the etching process. Although, in general, the secondary ion efficiency of the hydrogen atom is higher than that of the heavy hydrogen atom, the stronger intensity of the deuterium ion, D^+, than that of the proton, H^+, was maintained during the etching of the polymer film. This stronger intensity of D^+ results from the larger fraction of heavy hydrogen atom in the end-labeled dPS. Figure 6 revealed an apparent increase in the intensity of H^+ and a decrease in that of D^+ in the air−polymer interface region. Since the styrene unit was deuterated, protons were present only in both chain end portions. Thus, the SIMS depth profile apparently shows a remarkable enrichment of chain end groups at the air−polymer interface. Since the surface localization of chain end groups induces the excess free volume fraction at the film surface compared with that in the bulk phase, it seems reasonable to conclude that the surface T_g is lower than the bulk T_g, resulting in molecular motion at the film surface being fairly active in comparison with that for the bulk sample at room temperature.

As shown in Figure 7, the localization decay length of chain end groups was defined as the range from the

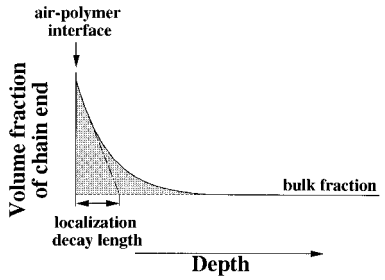

Figure 7. Definition of localization decay length.

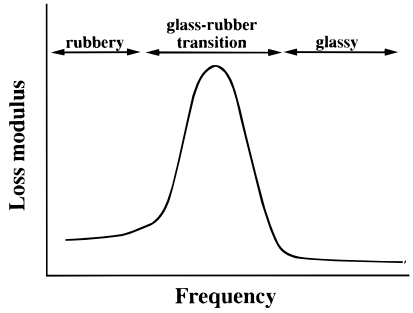

Figure 8. Schematic representation of the frequency dependence of dynamic loss modulus, E''.

air−polymer interface to the depth that the initial slope of the H^+ profile crossed the bulk intensity. The localization decay length of chain end groups was 4.4 nm and its value was almost comparable the radius of gyration of an unperturbed chain, R_g, of 3.3 nm.

Relaxation Behavior of Molecular Chains at the Film Surface. In order to investigate the relaxation behavior of molecular chains at the film surface, LFM measurements were carried out at 293 K. Figure 8 shows the schematic representation of frequency dependence of dynamic loss modulus, E'', for the polymeric solids.[29] In the case of very high or low frequency ranges, the polymer film is in a glassy state or a rubbery one, respectively, and has the low magnitude of E''. On the other hand, in an intermediate frequency region, the polymer film is in a glass−rubber transition state and, then, exhibits the peak of E''. Hereupon, we consider the scanning rate dependence of lateral force that directly corresponds to the frequency dependence of surface mechanical property, as shown in Figure 8. The frequency, f, is proportional to an inverse of a period, T

$$f = 1/T \tag{5}$$

and also, T can be expressed as

$$T = 2a/\nu \tag{6}$$

where a and ν are the contact radius and the scanning rate of the tip, respectively. According to Hertz' elastic theory, a can be expressed as follows.[24]

$$a = \left[\frac{3}{4}\left(\frac{1-\mu_{\text{tip}}{}^2}{E_{\text{tip}}} + \frac{1-\mu_{\text{polymer}}{}^2}{E_{\text{polymer}}}\right)RF_c\right]^{1/3} \tag{7}$$

As eqs 5 and 6 are substituted into eq 7, the relationship between frequency and scanning rate can be expressed as follows.

$$f = \frac{\nu}{2}\left[\frac{3}{4}\left(\frac{1-\mu_{\text{tip}}{}^2}{E_{\text{tip}}} + \frac{1-\mu_{\text{polymer}}{}^2}{E_{\text{polymer}}}\right)RF_c\right]^{-1/3} \tag{8}$$

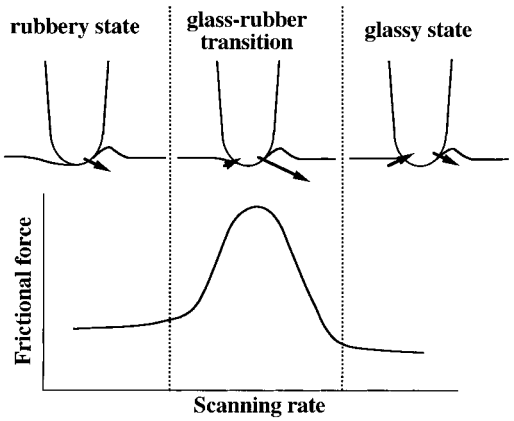

Figure 9. Schematic illustration of the deformed surface by a sliding tip. The length of an arrow shows the magnitude of energy impartation.

Then, the abscissa, f, of Figure 8 can be replaced by the scanning rate, ν.

Next, the relationship between E'' and lateral force will be discussed. Figure 9 shows the schematic illustration of the surface deformed by a sliding tip. When the tip slides on the polymer surface, the rim is produced ahead of the tip, as shown in the upper part of Figure 9. In the case of the glassy surface, elastic energy is stored in the front rim. However, since the relaxation time is very short, the deformed surface behind a sliding tip is quickly recovered and, then, elastic energy is imparted to a sliding tip. As a consequence, this leads to the total energy loss being small; that is, the frictional force is small. When the surface is in a rubbery state, the amount of energy to produce the front rim is small due to its small magnitude of E'. Even though the deformed surface behind a sliding tip cannot be relaxed quickly because of its long relaxation time, frictional force becomes small because of the small magnitude of E'. On the other hand, when the surface is in a glass−rubber transition state, the energy required for the formation of the front rim is larger than that for the glassy or rubbery state due to its large E''. Moreover, the deformed surface does not relax quickly. Therefore, the magnitude of frictional force becomes larger. Since the magnitude of frictional force is almost proportional to loss modulus, as mentioned previously in Figure 8, the E'' ordinate in Figure 8 can be replaced by the frictional force, as shown in the lower part of Figure 9.

Figure 10 shows the plots of lateral force against the scanning rate as a function of M_n. The tip indent depth of ca. 1.1 nm was comparable to the magnitude of static deformation for the forced modulation SFM measurement. The broken arrow in the figure denotes the scanning rate corresponding to the frequency of the forced modulation SFM measurement, which was calculated by eq 8. Lateral force measured by LFM is the sum of frictional force and adhesion force.[21] Since the scanning rate dependence of adhesion force is negligible,[30] the scanning rate dependence of lateral force indicates that frictional force strongly depends on the scanning rate. In the case of M_n of 140.0k, since the distinct scanning rate dependence of lateral force was not observed, it seems reasonable to conclude that the surface is in a glassy state. On the other hand, the lateral force for the PS film surface with M_n less than 40.4k was apparently dependent on the scanning rate. In the case of M_n of 40.4k, although the scanning rate dependence of lateral force was not observed at a high

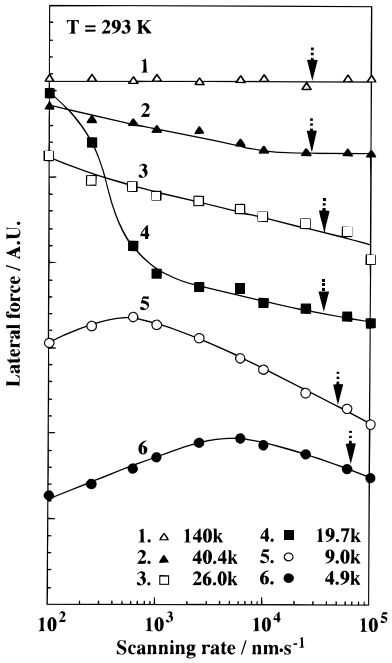

Figure 10. Scanning rate dependence of lateral force as a function of the number-average molecular weight. The broken arrow shows the scanning rate corresponding to the frequency of the forced modulation SFM measurement.

scanning rate region, the magnitude of lateral force was affected by the scanning rate at a low scanning rate region. Then, LFM measurement for the PS film with M_n of 40.4k at low and high scanning rates exhibits clearly the existence of a glass−rubber transition state and a glassy one, respectively. Since forced modulation SFM measurement for the PS film with M_n of 40.4k was performed at 4 kHz corresponding to the high scanning rate of 2.7×10^4 nm·s^{-1}, the surface E' of 4.5 GPa was quite reasonable. In the case of M_n of 26.6k and 19.7k, since lateral force decreased with an increase in scanning rate, it can be concluded that the surface is in a glass−rubber transition state at 293 K. Moreover, in the case of M_n of 9.0k and 4.9k, the peak of lateral force was clearly observed on the lateral force-scanning rate curve. These results indicate that surface E'' has the maximum value in the scanning rate region employed in this study; that is, the surface of the PS film with M_n of 9.0k and 4.9k is in a glass−rubber transition state at 293 K. Since the surface T_g for the PS film with M_n of 9.0k is higher than that for the film with M_n of 4.9k, it is reasonable that the peak on the lateral force−scanning rate curve for the PS film with M_n of 9.0k appears in a lower scanning rate region in comparison with that for M_n of 4.9k.

Conclusion

Surface molecular motion for the monodisperse PS film was investigated on the basis of forced modulation SFM and LFM measurements. In the case of M_n less than ca. 30k, it was revealed that the film surface was in a glass−rubber transition state even at 293 K. A depression of the surface T_g compared with that for the bulk sample was explained by the surface localization of chain end groups. DSIMS measurement revealed that chain end groups were enriched in the depth range from the outermost surface to R_g.

Acknowledgment. This work was partially supported by Research Fellowships of the Japan Society for the Promotion of Science for Young Scientists.

References and Notes

(1) Meyers, G. F.; DeKoven, B. M.; Seitz, J. T. *Langmuir* **1992**, *8*, 2330.
(2) Keddie, J. L.; Jones, R. A. L.; Cory, R. A. *Europhys. Lett.* **1993**, *23*, 579.
(3) Keddie, J. L.; Jones, R. A. L. *Isr. J. Chem.* **1995**, *35*, 21.
(4) Reiter, G. *Langmuir* **1993**, *9*, 1344.
(5) Reiter, G. *Macromolecules* **1994**, *27*, 3046.
(6) Mayes, A. M. *Macromolecules* **1994**, *27*, 3114.
(7) Kajiyama, T.; Tanaka, K.; Ohki, I.; Ge, S.-R.; Yoon, J.-S.; Takahara, A. *Macromolecules* **1994**, *27*, 7932.
(8) Kajiyama, T.; Tanaka, K.; Takahara, A. *Macromolecules* **1995**, *28*, 3482.
(9) Tanaka, K.; Takahara, A.; Kajiyama, T. *Acta Polym.* **1995**, *46*, 476.
(10) Binnig, G.; Quate, C. F.; Gerber, C. G. *Phys. Rev. Lett.* **1986**, *56*, 930.
(11) Guntherrodt, H.-H.; Wiesendanger, R. *Scanning Tunneling Microscopy*; Springer-Verlag: New York, 1992−1993; Vols. I−III.
(12) Marti, O., Amrein, M., Eds. *STM and SFM in Biology*; Academic Press: New York, 1993.
(13) Maivald, P.; Butt, H. J.; Gould, S. A. C.; Prater, C. B.; Drake, B.; Gurley, J. A.; Elings, V. B.; Hansma, P. K. *Nanotechnology* **1991**, *2*, 103.
(14) Radmacher, M.; Tillmann, R. W.; Gaub, E. *Biophys. J.* **1993**, *64*, 735.
(15) Overney, R. M.; Meyer, E.; Frommer, J.; Guntherodt, H.-J.; Fujihira, M.; Takano, H.; Gotoh, Y. *Langmuir* **1994**, *10*, 1281.
(16) Overney, R. M. *Trends Polym. Sci.* **1995**, *3*, 359.
(17) Tanaka, K.; Yoon, J.-S.; Takahara, A.; Kajiyama, T. *Macromolecules* **1995**, *28*, 934.
(18) Ge, S.-R.; Takahara, A.; Kajiyama, T. *J. Vac. Sci. Technol.* **1994**, *A12*, 2530.
(19) Ge, S.-R.; Takahara, A.; Kajiyama, T. *Langmuir* **1995**, *11*, 1341.
(20) Overney, R.; Meyer, E.; Frommer, J.; Brodbeck, D.; Howald, L.; Guntherodt, H.; Fujihira, M.; Takano, H.; Gotoh, Y. *Nature* **1992**, *359*, 133.
(21) Koleske, D. D.; Barger, W. R.; Colton, R. J. *AVS National Symp. Abstr., 42nd* **1995**, NS+SS-TuA6.
(22) Grosch, K. A. *Proc. R. Soc. London A* **1963**, *274*, 21.
(23) Minato, K.; Takemura, T. *Jpn. J. Appl. Phys.* **1967**, *6*, 719.
(24) Haugstad, G.; Gladfelter, W. L.; Weberg, E. B.; Weberg, R. T.; Jones, R. R. *Langmuir* **1995**, *11*, 3473.
(25) Wiesendanger, R. *Scanning Probe Microscopy and Spectroscopy-Methods and Applications*; Cambridge University Press: New York, 1994.
(26) Tanaka, K.; Takahara, A.; Kajiyama, T. *Kobunshi Ronbunshu* **1996**, *53*, 582.
(27) Hertz, H. *J. Reine Angew. Math.* **1882**, *92*, 156.
(28) Naganuma, S.; Sakurai, T.; Takahashi, Y.; Takahashi, S. *Kobunshi Kagaku* **1972**, *29*, 105.
(29) Ward, I. M.; Hadley, D. W. *An Introduction to the Mechanical Properties of Solid Polymers*; John Wiley & Sons: Chichester, U.K., 1993.
(30) In order to investigate the scanning rate dependence of the adhesion force, the LFM measurement of the silicon wafer, which did not show viscoelastic properties and any scanning rate dependence of frictional force, was carried out under the same conditions as measurement of the monodisperse PS film. Since the scanning rate dependence of the lateral force was not observed, it seemed reasonable to conclude that the scanning rate dependence of the adhesion force was negligible in this scanning rate region.

MA960582Y